Exponentially decaying interaction potential of cavity solitons

Exponentially decaying interaction potential of cavity solitons

Shayesteh Rahmani Anbardan,[1,2] Cristina Rimoldi,[3,*] Reza Kheradmand,[1,†] Giovanna Tissoni,[3] and Franco Prati[2]
[1]*Photonics Group, RIAPA, University of Tabriz, Tabriz, Iran*
[2]*Dipartimento di Scienza e Alta Tecnologia, Università dell'Insubria, Via Valleggio 11, 22100 Como, Italy*
[3]*Université Côte d'Azur, CNRS, Institut de Physique de Nice, Valbonne, France*

(Received 21 August 2017; revised manuscript received 29 January 2018; published 20 March 2018)

We analyze the interaction of two cavity solitons in an optically injected vertical cavity surface emitting laser above threshold. We show that they experience an attractive force even when their distance is much larger than their diameter, and eventually they merge. Since the merging time depends exponentially on the initial distance, we suggest that the attraction could be associated with an exponentially decaying interaction potential, similarly to what is found for hydrophobic materials. We also show that the merging time is simply related to the characteristic times of the laser, photon lifetime, and carrier lifetime.

DOI: 10.1103/PhysRevE.97.032208

I. INTRODUCTION

It is well known that high-dimensional optical dynamics, which arise from the competition of a large number of spatial and/or temporal degrees of freedom, present several analogies to hydrodynamics [1,2]. Optical vortices [3], turbulence [4], photon flux along channels [5], and rogue waves [6–8] are just some examples. In the subfield of localized structures, striking similarities were shown between the trajectories of confined self-propelled cavity solitons in a laser with saturable absorber [9] and those of the so-called walkers, droplets bouncing over a vessel containing the same liquid, which vibrates vertically close to the Faraday instability threshold [10].

In this paper we add a piece to the puzzle, suggesting that two cavity solitons in an optically driven laser interact in a way similar to that of hydrophobic materials, i.e., with an exponentially decaying interaction potential [11]. The hydrophobic force is the unusually strong attraction (much stronger than van der Waals force) experienced by nonpolar molecules and surfaces in water, and it is ubiquitous in water-based systems and in everyday life [12].

Cavity solitons (CSs) are self-confined light beams which form in optical cavities where some particular mechanism compensates for diffraction or dispersion [13,14]. Since one of the main applicative interests of CSs is bitwise information encoding (1 if the CS is present, 0 if it is absent), it is of fundamental importance to know how they interact in order to determine how many independent CSs can be stored in a cavity. The existence of a critical distance above which two CSs behave as independent entities determines the maximum information density of a particular device. In this respect, a further distinction can be introduced between temporal (propagating) CSs and spatial CSs.

Temporal CSs have attracted much interest since it was realized that their frequency-domain counterparts are frequency combs that can span large portions of an octave [15]. From the viewpoint of information storage, it was shown that in a fiber laser the critical temporal distance above which two CSs no longer interact is about 40 ps, which implies that the information storage density is 125 bits/m [16]. In those studies the resonator is passive and it is driven by a coherent external field. A new kind of temporal CS has been demonstrated more recently that forms in an active resonator, a highly multi-longitudinal-mode ring laser, again driven by a coherent external field [17]. These CSs were named phase solitons because they are associated with a 2π rotation of the electric field in the Argand plane which gives them a chiral charge. Unlike temporal CSs in fiber resonators, phase solitons display long range interaction, which ultimately leads to the formation of complexes with multiple chiral charge [18].

Spatial CSs have been mainly studied in semiconductor-based devices, whose capacity is of course much more limited because even the largest samples have a transverse size of at most a few hundred micrometers. They were first demonstrated in coherently driven semiconductor lasers below threshold [19,20]. Earlier theoretical studies about interactions of CSs have been made in the case where the nonlinear medium was a collection of passive two-level atoms [21,22], that is, without population inversion. The existence of two critical distances was demonstrated, let us call them d_1 and d_2, such that if two CSs are created with an initial distance smaller than d_1 they merge or annihilate, if the initial distance is larger than d_2 they do not interact, and if the initial distance is in between they repel until they reach the distance d_2. Those results were basically confirmed in a later work based on a more refined bulk semiconductor model, with the difference that if the initial distance is in between d_1 and d_2 the two CSs may either attract or repel until the distance is equal to a third value, d^*, with $d_1 < d^* < d_2$. In addition, depending on the sign of the frequency detuning between the injected field and the medium resonance, more than one equilibrium distance may exist, related to the presence of tails in the soliton intensity profile [23].

*Present address: INRS-EMT, 1650 Boulevard Lionel-Boulet, Varennes, Québec J3X 1S2, Canada.
†r.kheradmand.a@gmail.com

Although it was later demonstrated that spatial CSs exist also in driven semiconductor lasers, i.e., with the active medium pumped above the laser threshold [24], no further systematic studies of the interaction of CSs in those configurations were carried out. A possible reason for that is that it became immediately evident that real devices are far from being transversely homogeneous, especially when the medium is pumped, and the CSs are pinned to particular points of the transverse section (defects) [25]. Nevertheless, it is also true that the influence of parameter gradients or material defects can be overcome thanks to an external periodic modulation, allowing for the creation of a regular array where CSs are placed in well-controlled equilibrium positions [26].

In this paper we show that the interaction of CSs in a driven laser is fundamentally different from that of a driven passive resonator, and it rather presents striking analogies with hydrodynamics.

II. MODEL

We study the interaction of two CSs in a vertical cavity surface emitting laser (VCSEL)-type laser with incoherent pump and coherent optical injection as schematically illustrated in Fig. 1 [24]. The geometry of the VCSEL guarantees a broad two-dimensional cross section, which makes soliton interaction independent of the boundary conditions, and restricts the dynamics to a single longitudinal mode, thus simplifying the model equations.

We consider the following set of effective Maxwell-Bloch equations [24,27]:

$$\partial_t E = \sigma[E_I - (1+i\theta)E + P + i\nabla^2 E], \tag{1}$$

$$\partial_t D = J - D - (E^* P + E P^*)/2 + d\nabla^2 D, \tag{2}$$

$$\partial_t P = \xi(D)[(1-i\alpha)f(D)E - P], \tag{3}$$

where E and P are the slowly varying electric field and effective material polarization, respectively, D is the carrier density, σ is the ratio of carrier lifetime τ_c to photon lifetime τ_{ph}, E_I is the injected field amplitude, θ is the frequency detuning between cavity and optical injection multiplied by the photon lifetime, α is the linewidth enhancement factor, J is the pump (electric or optical), and d is the carrier diffusion constant.

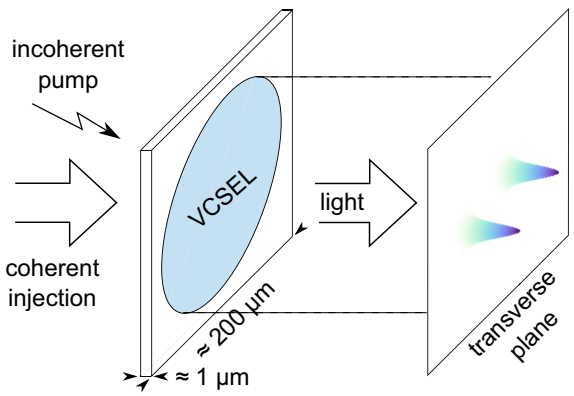

FIG. 1. Sketch of the VCSEL with optical injection and incoherent pump, with the typical dimensions and a three-dimensional image of the interacting solitons

Diffraction is described by the transverse Laplacian operator, ∇^2, and time is scaled to τ_c (typically of order 1 ns), while the spatial scale is the square root of the diffraction parameter.

The real function $f(D)$ accounts for the nonlinearity of gain typical of quantum wells [27]. Assuming that the nonlinearity is quadratic we set $f(D) = (1-\beta D)D$, with $\beta = 0.125$, a value obtained as the best fit of the gain calculated with a microscopic model [27]. Nonlinearity implies that the threshold current for the free running laser is different from 1 and we have $J_{\rm th} = (1-\sqrt{1-4\beta})/(2\beta)$. With our choice of β, the threshold current is $J_{th} = 1.17$.

The complex function $\xi(D)$ in the equation for the macroscopic polarization accounts for the dependence on the carrier density of the gain linewidth and of the position of the frequency where gain is a maximum [24].

In a laser with optical injection when the frequency of the external field is not exactly matched to that of the solitary laser no stable states exist as long as the amplitude y of the injected field is smaller than a critical value (injection locking point). The laser output is oscillatory and, in a two-dimensional system like ours, several transverse modes can be excited. Under those conditions the dynamical equation for the macroscopic polarization P acts as a spectral filter, because it includes the effect of the finite gain linewidth, and it is necessary to avoid nonphysical short wavelength instabilities.

In this paper, however, we focus on the interaction of cavity solitons that exist beyond the injection locking point and this enables us to use the reduced set of equations

$$\partial_t E = \sigma[E_I - (1+i\theta)E + (1-i\alpha)f(D)E + i\nabla^2 E], \tag{4}$$

$$\partial_t D = J - D - f(D)|E|^2 + d\nabla^2 D, \tag{5}$$

which are obtained with a standard adiabatic elimination of P [28]. In the simulations we kept fixed the parameters $J = 1.2J_{\rm th}$, $\alpha = 4$, $\theta = -2$, $d = 0.052$, and $E_I = 1$, and varied only σ. These are typical parameters already used to model experiments about CSs in a laser with optical injection above threshold [24]. In particular, the chosen value of the diffusion parameter is for a diffusion length of about 1 μm. With these parameters a CS with a stationary background is stable, with radius (HWHM) approximately equal to one space unit.

III. DYNAMICS OF MERGING SOLITONS

Our simulations simply consisted of switching on at the same time two CSs at a certain initial distance r_0 and seeing what happens. We observed that even when r_0 is of the order of 10 space units, i.e., much larger than one soliton diameter, the two CSs experience an attractive force which makes them move toward each other and finally merge, forming a single CS.

Figure 2 shows the time evolution of CSs' distance for different initial values: the motion is very slow at the beginning, especially for the larger initial distances, and extremely fast at the end, just before merging. The fact that the interval between two consequent merging times is approximately constant in a logarithmic scale suggests that the merging time depends exponentially on the initial distance. The assumption is substantially confirmed by the plot of Fig. 3, although the points are not perfectly aligned on a straight line.

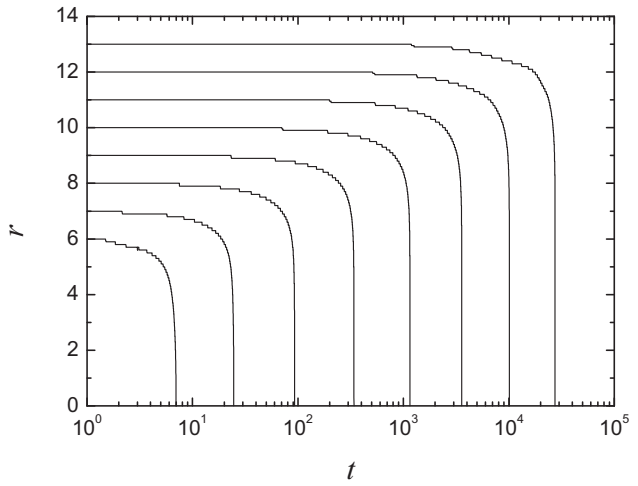

FIG. 2. Time evolution of solitons' distance for different initial values and $\sigma = 400$.

We remark that an exponential dependence of the merging time on the initial distance has been recently observed also for phase solitons, although in that case the final structure is different from the initial ones, being a soliton with double chiral charge [18].

We interpreted these data as a further manifestation of the particle-like character of CSs. It is known that the merging time of two masses under the gravitational potential r^{-1} scales as $r_0^{3/2}$, if r_0 is the initial distance [29]. By analogy, we assumed that a merging time which increases exponentially with the initial distance is associated with an interaction potential which decreases exponentially with the distance, such as

$$V(r) = -K^2 \mathrm{e}^{-r/R}. \tag{6}$$

The potential depends on two parameters: the strength K and the range R. Effective potentials are often introduced to describe the particle-like interaction of dissipative solitons and in particular to find the equilibrium distance in bound states [30–32].

Here we propose to extend the idea to the free fall motion of one soliton toward the other. To that aim we assume that the motion of the two CSs, regarded as particles moving in a potential, is conservative. If the two bodies are initially at rest at the distance r_0 and we set the unknown mass of the particle equal to 2, energy conservation implies that the velocity at a given distance $0 \leqslant x \leqslant r_0$ is $v(x) = -K\sqrt{e^{-x/R} - e^{-r_0/R}}$. Incidentally, this means that the parameter K has also the meaning of impact velocity in the limit $r_0 \gg R$. From the expression for the velocity we can calculate the time needed to reach the distance r as

$$t(r) = \int_r^{r_0} \frac{dx}{v(x)} = \frac{2R}{K} e^{r_0/(2R)} \arctan\sqrt{e^{(r_0-r)/R} - 1}. \tag{7}$$

It follows that the merging time $t_m = t(0)$ is

$$t_m = \frac{2R}{K} e^{r_0/(2R)} \arctan\sqrt{e^{r_0/R} - 1}. \tag{8}$$

Even if the initial distance r_0 is just a few times the interaction range R the arctangent can be replaced by $\pi/2$ and we have a simple approximated exponential law for the merging time:

$$t_{m,ap} = \pi \frac{R}{K} e^{r_0/(2R)}. \tag{9}$$

The straight line in Fig. 3 is a fit of the numerical data obtained discarding those for which $r_0 < 10$, in accordance with the fact that Eq. (9) is strictly valid only in the limit of large initial distances. The slope of the linear fit allows one to determine with high precision the value of the R parameter as $R = 0.474$, about one-half the soliton radius, showing that the potential is actually short ranged.

If both R and K are known we can obtain the complete time evolution of the distance by (graphically) inverting Eq. (7). Unfortunately, the uncertainty in the intercept of the linear fit is much larger than that of the slope and thus a precise estimation

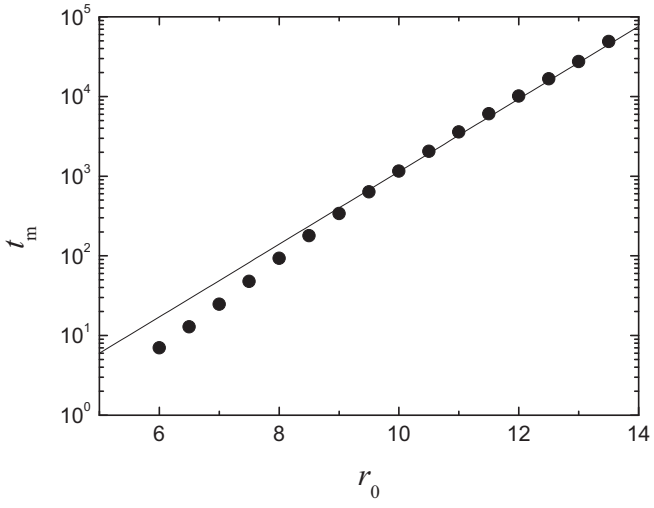

FIG. 3. Semilogarithmic plot of the merging time of two cavity solitons as a function of their initial distance for $\sigma = 400$. The straight line has equation $y = a + bx$, with $a = -3.460 \pm 0.12$ and $b = 1.055 \pm 0.01$, and it was obtained as a fit of the eight largest initial distances, from $r_0 = 10$ to $r_0 = 13.5$.

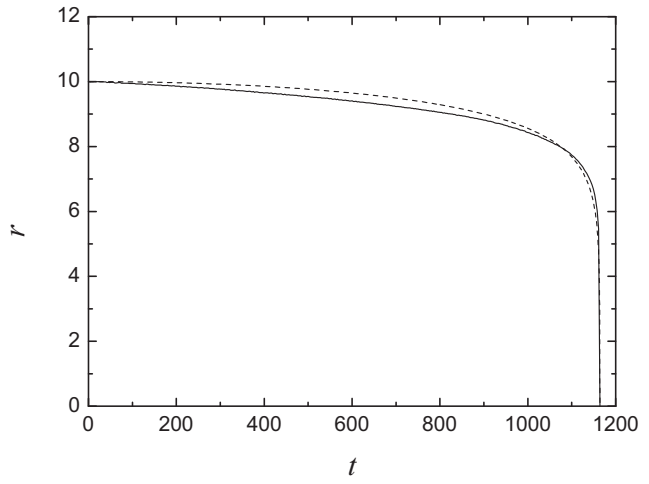

FIG. 4. Time evolution of solitons' distance for $\sigma = 400$ and $r_0 = 10$. The solid line is the numerical simulation; the dashed line is the analytic curve given by Eq. (7) with $R = 0.474$ and $K = 48.77$.

of the interaction strength K is not possible. In Fig. 4 the comparison between the numerically calculated distance and the analytic curve for the initial distance $r_0 = 10$ is made assuming $K = 48.77$, which corresponds to the intercept $a = -3.382$, a value compatible with the uncertainty of the fit, chosen in such a way that the duration of the motion is the same for both curves. The analytic curve reproduces well the exact time dependence of the distance; the larger deviations are observed in the central stage of the motion, but they remain smaller than 3%. For instance, at $t = 700$ the distance in the numerical simulation is $r = 9.493$ and the theoretical one is $r = 9.235$.

IV. DEPENDENCE OF THE MERGING TIME ON PHOTON AND CARRIER LIFETIMES

In the above simulations we kept fixed the decay rate $\sigma = \tau_c/\tau_{ph} = 400$, which amounts to assuming that photons are 400 times faster than carriers, a typical value for a semiconductor microresonator. In order to determine if and how that ratio influences the interaction strength we made other simulations with $\sigma = 40$, 4, and 1, which would correspond to progressively longer (external) resonators. Since the results for $\sigma = 40$ differ very little from those with $\sigma = 400$, we focused on the two sets of simulations with the smaller σ. In Fig. 5 we display together the three fits of the merging time for $\sigma = 400$, 4, and 1. The slope is the same for all three; we only observe an upward shift of the three lines for decreasing σ, which means that the merging time increases with the photon lifetime. We conclude that the range R of the interaction potential, which is related to the slope, is independent of σ, whereas the interaction strength K decreases with σ. However, it is not reasonable to assume a particular functional dependence of K on σ because, as mentioned above, the uncertainty of the values of K given by the fit is too large.

Finally, in Fig. 6 we show how the merging times for different initial distances depend on σ^{-1}. The dependence is clearly linear, and we found that in general we can write

$$t_m(r_0) = f(r_0)\left(1 + \frac{\eta}{\sigma}\right). \tag{10}$$

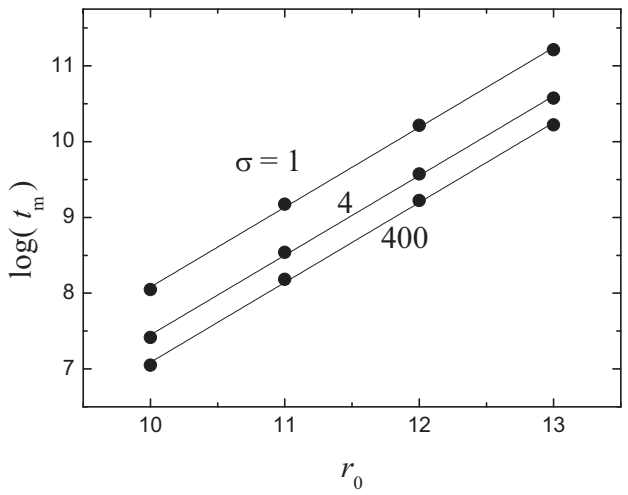

FIG. 5. Semilogarithmic plot of the merging time of two cavity solitons as a function of their initial distance for different values of the relative decay rate σ.

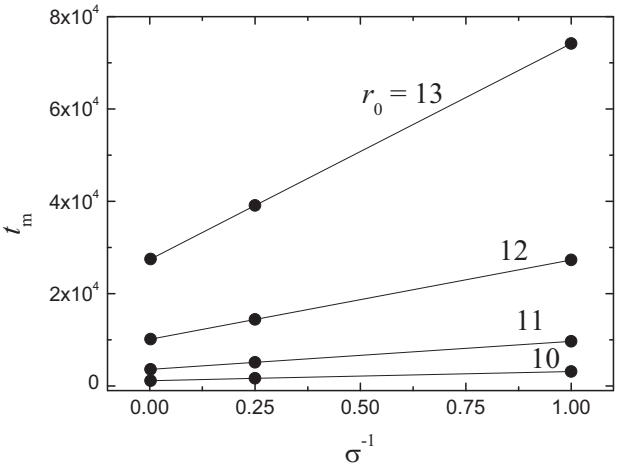

FIG. 6. Merging time of two cavity solitons as a function of the inverse of the relative decay rate σ for different values of the initial distance r_0.

The function $f(r_0)$ represents the limit value of the merging time for photon lifetime approaching zero and it can be estimated as $f(r_0) = 0.0321e^{1.053r_0}$. A comparison with Eq. (9) shows that $R \simeq 0.474$, as before, and $K \simeq 46.4$. The latter is the maximum value of the interaction strength and also the maximum possible impact velocity. Assuming that one space unit is 4 μm and one time unit is 1 ns, this amounts to a maximum impact velocity of about 200 μm/ns = 200 km/s, at least one order of magnitude larger than the average velocities measured for a CS set in motion by a phase gradient [33].

The parameter η turns out to be independent of r_0, because for the four lines considered we got $\eta = 1.7 \pm 0.008$. Since time t is the physical time τ scaled to τ_c and $\sigma = \tau_c/\tau_{ph}$ we have for the physical merging time

$$\tau_m(r_0) = f(r_0)(\tau_c + 1.7\tau_{ph}). \tag{11}$$

V. CONCLUSIONS

In conclusion, we have demonstrated that in an optically injected VCSEL above threshold cavity solitons experience an attractive force even at distances much larger than their diameter. Due to that attraction the solitons move toward each other with increasing velocity and finally merge. The merging time with good approximation depends exponentially on the initial distance.

We interpreted the above results as the conservative motion of two particles subject to an exponentially decaying potential, similar to that experienced by hydrophobic materials in water. This is again in contrast with the overdamped dynamics of cavity solitons in passive resonators, where it was shown that the interaction of two nearby solitons causes a non-Newtonian motion where the velocity, rather than the acceleration, is proportional to the perturbation produced by one soliton on the other [32].

The physical explanation that can be found in the literature for the interaction of solitons is that a force acts on each soliton due to the presence of its mate. In simple models where the dynamics is governed by a single equation for the electric field, a perturbative approach is possible which allows one to derive

analytical expressions for the interaction potential. Such simple models include the nonlinear Schrödinger equation [30], the parametrically driven Ginzburg-Landau equation [31], and the Maxwell equation for a driven resonator containing a nonlinear absorber [32].

Our system is intrinsically more complex. Since we are considering a class-B laser with optical injection, the model must include also an equation for the dynamics of the gain, and this prevents us from performing an analytical study of the same kind as those reported above. Hence, we can only infer from the dynamics what is a possible form of the interaction potential.

The results show that the interaction of solitons in a class-B laser is certainly mediated by the gain medium, since the merging time depends on the carrier recombination time as well as the photon lifetime.

Our findings contrast with those reported in passive resonators, where it was shown that two cavity solitons which are initially set sufficiently apart from each other never merge.

An explanation for the different behavior is that in passive resonators cavity solitons are characterized by diffractive tails in their intensity profiles, with an alternation of maxima and minima. Therefore, the interaction potential of two distant solitons is also oscillatory in space and several equilibria positions exist in correspondence with the minima. In the active case, instead, the cavity solitons do not present any oscillating tail, and this makes reasonable our choice of a monotonic potential. The different shapes of the intensity profiles in the two cases can be associated with the different shapes of the carrier density profiles, which present a bump and a dip, respectively, in the passive and active cases.

Phase solitons with the same chiral charge in a longitudinally extended driven semiconductor laser were also shown to experience an attractive force [18] which makes them collide and produce a single soliton after a merging time which increases exponentially with the initial distance. An important difference, however, is that the final soliton differs from the initial ones because it possesses a double chiral charge; i.e., the total charge is conserved.

ACKNOWLEDGMENTS

S.R.A. and R.K acknowledge support by the Center for International Scientific Studies & Collaborations (CISSC), Islamic Republic of Iran.

[1] M. Brambilla, L. A. Lugiato, V. Penna, F. Prati, C. Tamm, and C. O. Weiss, Phys. Rev. A **43**, 5114 (1991).
[2] K. Staliunas, Phys. Rev. A **48**, 1573 (1993).
[3] P. Coullet, L. Gil, and F. Rocca, Opt. Commun. **73**, 403 (1989).
[4] F. T. Arecchi, Phys. D **51**, 450 (1991).
[5] M. Vaupel, K. Staliunas, and C. O. Weiss, Phys. Rev. A **54**, 880 (1996).
[6] D. Solli, C. Ropers, P. Koonath, and B. Jalali, Nature (London) **450**, 1054 (2007).
[7] M. Onorato, S. Residori, U. Bortolozzo, A. Montina, and F. T. Arecchi, Phys. Rep. **528**, 47 (2013).
[8] J. M. Dudley, F. Dias, M. Erkintalo, and G. Genty, Nat. Photonics **8**, 755 (2014).
[9] F. Prati, L. A. Lugiato, G. Tissoni, and M. Brambilla, Phys. Rev. A **84**, 053852 (2011).
[10] S. Protiére, A. Boudaoud, and Y. Couder, J. Fluid Mech. **554**, 85 (2006).
[11] J. Israelachvili and R. Pashley, Nature (London) **300**, 341 (1982).
[12] S. Donaldson, A. Røyne, K. Kristiansen, M. Rapp, S. Das, M. Gebbie, D. Lee, P. Stock, M. Valtiner, and J. Israelachvili, Langmuir **31**, 2051 (2015).
[13] L. Lugiato, F. Prati, and M. Brambilla, *Nonlinear Optical Systems* (Cambridge University Press, Cambridge, U.K., 2015).
[14] T. Ackemann, W. J. Firth, and G.-L. Oppo, Adv. At. Mol. Opt. Phys. **57**, 323 (2009).
[15] P. Del'Haye, A. Schliesser, O. Arcizet, T. Wilken, R. Holzwarth, and T. Kippenberg, Nature (London) **450**, 1214 (2007).
[16] F. Leo, S. Coen, P. Kockaert, S.-P. Gorza, P. Emplit, and M. Haelterman, Nat. Photonics **4**, 471 (2010).
[17] F. Gustave, L. Columbo, G. Tissoni, M. Brambilla, F. Prati, B. Kelleher, B. Tykalewicz, and S. Barland, Phys. Rev. Lett. **115**, 043902 (2015).
[18] F. Gustave, C. Rimoldi, P. Walczak, L. Columbo, M. Brambilla, F. Prati, G. Tissoni, and S. Barland, Eur. Phys. J. D **71**, 154 (2017).
[19] S. Barland, J. Tredicce, M. Brambilla, L. Lugiato, S. Balle, M. Giudici, T. Maggipinto, L. Spinelli, G. Tissoni, T. Knödl *et al.*, Nature (London) **419**, 699 (2002).
[20] X. Hachair, S. Barland, L. Furfaro, M. Giudici, S. Balle, J. Tredicce, M. Brambilla, T. Maggipinto, I. Perrini, G. Tissoni *et al.*, Phys. Rev. A **69**, 043817 (2004).
[21] N. Rosanov and G. Khodova, J. Opt. Soc. Am. B **7**, 1057 (1990).
[22] M. Brambilla, L. Lugiato, and M. Stefani, Chaos **6**, 368 (1996).
[23] G. Tissoni, L. Spinelli, M. Brambilla, T. Maggipinto, I. Perrini, and L. Lugiato, J. Opt. Soc. Am. B **16**, 2095 (1999).
[24] X. Hachair, F. Pedaci, E. Caboche, S. Barland, M. Giudici, J. Tredicce, F. Prati, G. Tissoni, R. Kheradmand, L. Lugiato *et al.*, IEEE J. Sel. Top. Quantum Electron. **12**, 339 (2006).
[25] F. Pedaci, G. Tissoni, S. Barland, M. Giudici, and J. Tredicce, App. Phys. Lett. **93**, 111104 (2008).
[26] F. Pedaci, P. Genevet, S. Barland, M. Giudici, and J. Tredicce, Appl. Phys. Lett. **89**, 221111 (2006).
[27] M. Eslami, R. Kheradmand, and G. Hashemvand, Opt. Quantum Electron. **46**, 319 (2014).
[28] F. Prati, G. Tissoni, C. McIntyre, and G. L. Oppo, Eur. Phys. J. D **59**, 139 (2010).
[29] S. K. Foong, Eur. J. Phys. **29**, 987 (2008).
[30] B. A. Malomed, Phys. Rev. E **47**, 2874 (1993).
[31] B. Malomed and A. Nepomnyashchy, Europhys. Lett. **27**, 649 (1994).
[32] A. G. Vladimirov, J. M. McSloy, D. V. Skryabin, and W. J. Firth, Phys. Rev. E **65**, 046606 (2002).
[33] F. Pedaci, S. Barland, E. Caboche, P. Genevet, M. Giudici, J. Tredicce, T. Ackemann, A. Scroggie, W. Firth, G.-L. Oppo *et al.*, Appl. Phys. Lett. **92**, 011101 (2008).